PCCP

Cite this: *Phys. Chem. Chem. Phys.*, 2011, **13**, 10111–10118

www.rsc.org/pccp

PAPER

A hybrid sol–gel synthesis of mesostructured SiC with tunable porosity and its application as a support for propane oxidative dehydrogenation†

Jie Xu,[a] Yong-Mei Liu,[b] Bing Xue,[a] Yong-Xin Li,*[a] Yong Cao*[b] and Kang-Nian Fan[b]

Received 17th December 2010, Accepted 10th March 2011
DOI: 10.1039/c0cp02895a

Porous silicon carbide (SiC) is of great potential as catalyst support in several industrially important reactions because of its unique thermophysical characteristics. Previously porous SiC was mostly obtained by a simple sol–gel or reactive replica technique which can only produce a material with low or medium surface area (< 50 m^2 g^{-1}). Here we report a new hybrid sol–gel approach to synthesize mesostructured SiC with high surface area (151–345 m^2 g^{-1}) and tunable porosity. The synthesis route involves a facile co-condensation of TEOS and alkyloxysilane with different alkyl-chain lengths followed by carbothermal reduction of the as-prepared alkyloxysilane precursors at 1350 °C. The resulting materials were investigated by X-ray diffraction, N_2 adsorption-desorption, transmission electron microscopy, scanning electron microscopy, and X-ray photoelectron spectroscopy. A mechanism for the tailored synthesis of mesostructured SiC was tentatively proposed. To demonstrate the catalytic application of these materials, vanadia were loaded on the mesostructured SiC supports, and their catalytic performance in oxidative dehydrogenation of propane was evaluated. Vanadia supported on the mesostructured silicon carbide exhibits higher selectivity to propylene than those on conventional supports such as Al_2O_3 and SiO_2 at the same propane conversion levels, mainly owing to its outstanding thermal conductivity which makes contributions to dissipate the heat generated from reaction thus alleviating the hot spots effect and over-oxidation of propylene.

1. Introduction

Silicon carbide (SiC) possesses unique properties such as high thermal conductivity, excellent thermal stability, mechanical strength, and chemical inertness.[1–3] These properties make SiC a suitable material for numerous applications in various fields, *e.g.* semi-conducting devices, biomaterials, and catalysis.[4–8] Due to these unique properties, much effort has also been devoted to the use of SiC as possible heterogeneous catalyst support in place of the classical supports such as alumina or silica, especially in highly endothermic and/or exothermic reactions.[9–12] In this context, the use of SiC as a catalyst support has been demonstrated for several reactions including, hydrodesulfurization,[13,14] automotive exhaust-pipe reactions,[9] hydrocarbon isomerization,[15] and the selective oxidation of butane into maleic anhydride.[16] Recently SiC was also successfully used as a support for ZSM-5 and BEA zeolites in methanol-to-olefins processes and Friedel–Crafts reactions.[17] In most cases, it is often desirable to have the SiC material with a high accessible specific area as well as a large and well developed porous texture.[1,3,18] Unfortunately, commercially available SiC materials generally have low surface areas, which are rather small compared to the typical silica or alumina supports or catalysts.[18]

Much effort has been devoted to the synthesis of porous SiC having a large surface area. So far, numerous technical methods including chemical vapor deposition (CVD),[19] direct carbonization of Si metals,[20] pyrolysis of organic or polymeric precursors,[21] and carbothermal reduction of a silica matrix[9] in the presence of an inert atmosphere have been developed to prepare porous SiC for various applications. Among the preparation methods, the carbothermal reduction of SiO_2 using carbon has attracted enormous interest,[22,23] because the cost of the raw materials is relatively low, they allow relatively low-temperature synthesis, the resulting materials are very pure, and they can retain the structure and morphology of the starting carbonaceous materials very well. Nevertheless, either the specific surface area (≤ 150 m^2 g^{-1}) or the porosity prepared by the above-mentioned methods is not satisfactory. Therefore, many attempts have been made to overcome these problems over the past decades, including the carbothermal reduction of a SiOC precursor derived by polysiloxane pyrolysis,[24]

[a] *College of Chemistry and Chemical Engineering, Changzhou University, Gehu Road 1, Changzhou, Jiangsu 213164, P. R. China. E-mail: liyxluck@126.com; Tel: (+86)-519-86330135*
[b] *Shanghai Key Laboratory of Molecular Catalysis and Innovative Materials, Department of Chemistry, Fudan University, Shanghai 200433, P. R. China. E-mail: yongcao@fudan.edu.cn; Tel: (+86)-21-55665287*
† Electronic supplementary information (ESI) available. See DOI: 10.1039/c0cp02895a

the use of periodic mesoporous silica with various mesophases as the silica source or the alternative use of sol–gel synthesis as a convenient and practical method for the introduction of silica precursor prior to the carbothermal reduction processing.[3,18,25–27] However, the high cost and complicated synthesis route impede the wide application of porous SiC materials.

In the continued search for more effective techniques for porous SiC fabrication, there is a definite need for new versatile method that can allow more convenient and economical preparation of catalytically attractive porous SiC materials. In this study, we report the development of a new practical hybrid sol–gel/carbothermal reduction approach to synthesize single-phase β-SiC materials with several desirable features including a large surface area as well as pore volume and a well-developed porosity in the mesoporous range. The resulting materials were investigated by X-ray diffraction (XRD), N_2 adsorption-desorption, transmission electron microscopy (TEM), scanning electron microscopy (SEM), and X-ray photoelectron spectroscopy (XPS). To demonstrate the applications, we load vanadia onto the as-synthesized mesoporous SiC, and investigate their catalytic activity in oxidative dehydrogenation (ODH) of propane. Our results have shown that mesoporous SiC are new attractive supports applicable for the fabrication of new promising V/SiC catalysts highly active and selective for the ODH of propane.

2. Experimental section

2.1 Synthesis of SiC

The mesostructured SiC materials were synthesized *via* a sol–gel process and carbonthermal reduction. 25 g of sucrose and 30 mL distilled water were dissolved in 50 mL ethanol at 50 °C. Subsequently, a given amount of TEOS (tetraethyl orthosilicate), alkyloxysilane (Table 1), and 10 mL oxalic acid solution (3.5 wt%) were added to the ethanol solution dropwise, followed by stirring until a gel was formed. Then, the gel was aged at 110 °C for 24 h to obtain a xerolgel. The resultant xerogel was calcined in an argon flow (40 mL min^{-1}) with the following temperature program: from room temperature to 800 °C with a ramp of 4 °C min^{-1}, and then to 1350 °C with a ramp of 2 °C min^{-1}, the temperature was kept at 1350 °C for 10 h.

The raw SiC product was immersed in the HF solution (20 wt%) under vigorous stirring for 24 h to remove unreacted silica and then calcined at 700 °C in air for 2–3 h to eliminate the residual carbon. Eventually, loose and greenish powders were obtained after washing with distilled water. The prepared mesostructured SiC materials with/without adding alkyloxysilane were designated as SiC-C_x (x represents the length of the alkyl chain of alkyloxysilane) and SiC-TEOS, respectively.

2.2 Preparation of catalysts

SiC-supported vanadia catalysts were prepared following the procedure described in our previous work:[28,29] SiC support was dispersed in a methanol solution of NH_4VO_3 at 60 °C. After evaporating the solvent at 120 °C overnight, the solid sample was calcined at 600 °C in static air for 2 h. The obtained samples were labeled as nV-SiC (n means the V content in the calcined catalysts) and summarized in Table 1. For comparison, vanadia catalysts supported on Al_2O_3 (~250 m^2 g^{-1}) and amorphous silica (~260 m^2 g^{-1}) were also prepared following the same procedure above. Additionally, to study the influence of the surface property of SiC materials on its catalytic behavior, freshly synthesized SiC was immersed into HF solution (40 wt%) for 24 h under vigorous stirring to remove the superficial silica film. The thus treated sample was named by adding suffix "-F" to original name.

2.3 Characterization

Structural analysis of SiC was carried out on a Bruker D8 Advance X-ray diffractometer equipped with a graphite monochromator, operating at 40 kV and 40 mA and employing nickel-filtered Cu-Kα radiation (λ = 1.5418 Å).

Nitrogen adsorption–desorption isotherms were generated at −196 °C with a Micromeritics TriStar 3000 after the samples were degassed (1.33×10^{-2} Pa) at 300 °C overnight. The specific surface area was calculated following the Brunauer–Emmet–Teller (BET) method, and pore size distribution was determined by the Barret–Joyner–Halenda (BJH) method.

High resolution transmission electron microscopy (HRTEM) analysis was carried out with a JEOL 2010 electron microscope operating at 200 kV. Before being transferred into the TEM chamber, the samples dispersed in ethanol were deposited onto a carbon-coated copper grid and then quickly moved into the vacuum evaporator.

Scanning electron microscopy (SEM) was recorded digitally on a Philips XL 30 microscope operating at 30 kV. Before being transferred into the SEM chamber, the samples dispersed in ethanol were deposited on the sample holder and then quickly moved into the vacuum evaporator (LDM-150D) in which a thin gold film was deposited after drying in vacuum.

X-ray photoelectron spectroscopy (XPS) data were measured using a Perkin-Elmer PHI 5000C spectrometer working in the constant analyzer energy mode with Mg-Kα radiation as the excitation source. The carbonaceous C 1s line (284.6 eV) was used as the reference to calibrate the binding energies (BE).

Temperature-programmed reduction (TPR) profiles were obtained on a homemade apparatus loaded with 25 mg of catalyst. The samples were pre-treated in flowing air at 600 °C

Table 1 Textural profiles of SiC materials

Sample	Alkyloxysilane	n(TEOS) /mol	n(alkyloxysilane) /mol	S_{BET} /m^2 g^{-1}	Pore volume /cm^3 g^{-1}	D_{pore}[a] /nm
SiC-TEOS	—	0.225	—	101	0.35	30.4
SiC-C_1	*methyl*-Si(OMe)$_3$	0.200	0.025	151	0.56	18.0
SiC-C_4	*i-butyl*-Si(OEt)$_3$	0.200	0.025	207	0.76	8.9
SiC-C_8	*n-octyl*-Si(OEt)$_3$	0.200	0.025	345	0.92	5.7
SiC-C_8-A	*n-octyl*-Si(OEt)$_3$	0.200	0.012	320	0.87	5.9
SiC-C_8–B	*n-octyl*-Si(OEt)$_3$	0.200	0.050	245	0.81	6.8

[a] The pore-size distribution (PSD) determined based on the BJH method.

for 2 h in order to ensure complete oxidation. Then the samples were cooled to room temperature in argon. Subsequently, the samples were heated to 700 °C with a ramp of 10 °C min^{-1} under an H_2/Ar mixture (H_2/Ar molar ratio of 5/95 and a total flow of 40 mL min^{-1}). The H_2 consumption was monitored using a TCD detector.

2.4 Catalytic tests

The catalytic properties of the samples were investigated in a fixed-bed quartz tubular flow reactor (5 mm inner diameter, 540 mm long) equipped with several gas flow lines with mass flow controllers to supply the feed, consisting of a mixture of $C_3H_8/O_2/N_2$ with a molar ratio of 1/1/4 (unless otherwise specified, the total flow was fixed at 30 mL min^{-1}). The temperature of reactor is controlled by a coaxial thermocouple placed at the center of the oven. An additional small diameter quartz tube with a thermocouple in it was used to test the temperature in the centre of the catalyst bed. Catalyst samples (W_{cat} = 50 mg, 60–80 mesh) were introduced into the reactor and conducted pretreatment at 600 °C for 2 h in the flow of O_2 (15 mL min^{-1}). The product was analyzed by on-line chromatography (Agilent GC 6820 equipped with Propark Q column for hydrocarbons and TDX-01 column for permanent gas analysis, coupled with FID and TCD detectors respectively). The carbon balance of the detected compounds is closed to 100% ± 5% and was additionally monitored by the CO_x content after catalytic combustion of organic species in a final total oxidation reactor.[30]

3. Results and discussion

3.1 Physicochemical properties of mesostructured SiC materials

The surface area and the other physical parameters of various SiC samples are summarized in Table 1. For the SiC-TEOS prepared *via* the conventional sol–gel method, the surface area and pore diameter are *ca.* 101 m^2 g^{-1} and 30.4 nm, respectively. After the addition of alkyloxysilane with hydrophobic alkyl chain, the pore size decreases drastically while the surface area and pore volume increase observably. When the hydrophobic alkyl chain of the alkyloxysilane employed is up to eight carbon atoms, namely SiC-C_8, the surface area increases to 345 m^2 g^{-1} and the pore size decreases to 5.7 nm. It is worth noting that, if *n*-hexade-Si(OMe)$_3$ employed, the resultant SiC material would present a large surface area of 653 m^2 g^{-1} and a pore size of 3.7 nm (Fig. S1†). Taking into account the mass transfer in the heterogeneous reaction, catalytic support should present a moderate pore size. In this sense, the *n-octyl*-Si(OEt)$_3$, with an appropriate length of eight carbon atoms, is the optimal choice. Furthermore, the effect of the molar ratio of TEOS/alkyloxysilane on the textural properties of the SiC samples was also investigated (Table 1). It is found that the ratio (*n*TEOS /*n*alkyloxysilane = 8) is the ratio of choice, considering a larger surface area of SiC material as catalytic support.

Fig. 1 presents the N_2 adsorption-desorption isotherms of the SiC samples. All SiC samples display the type IV adsorption curve with hysteresis loops, indicating the SiC materials

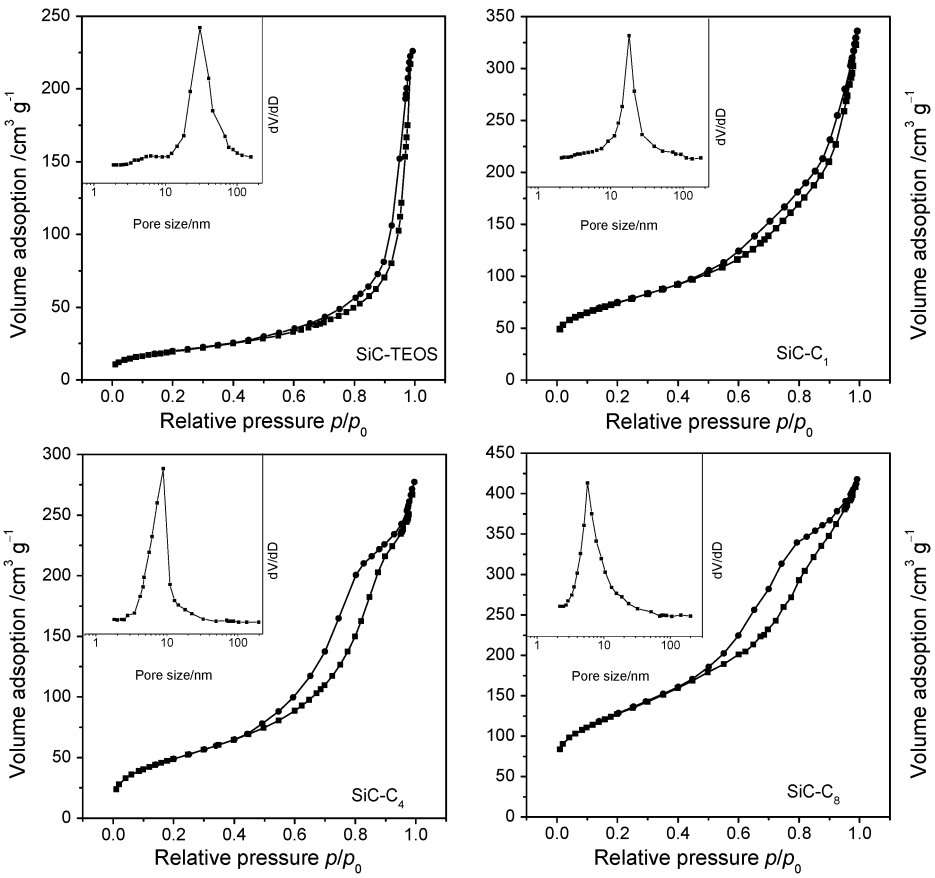

Fig. 1 N_2 adsorption-desorption isotherms and pore size distribution of SiC materials.

possess mesostructures. For SiC-TEOS sample, the isotherm still rises above the relative pressure of 0.9 p/p_0. This suggests that SiC-TEOS sample also presents some macroporous structure, for instance, interparticle or intrapaticle.[3,22,31] Meanwhile, the pore size distribution with a wide range of 10–60 nm confirms that some macroporous pores exist in the SiC-TEOS sample. In the case of the SiC-C_x materials, the hysteresis loops are limited in the medium relative pressure range of 0.5–0.9, along with comparably narrow pore size distributions, indicating that the pores of SiC-C_x materials present mesoporous structure exclusively.

XRD patterns of various SiC materials are presented in Fig. 2. The SiC-TEOS sample exhibits sharp and intense diffraction peaks at 2θ = 35.6°, 41.1°, 59.9° and 72.0°, corresponding to the (111), (200), (220), and (311) planes, respectively, which can be attributed to a typical face-centered cubic structure of β-SiC (JCPDS: 73–1665).[8,13,32] Calculated by Scherrer's equation (based on 111 plane), the average particle size of SiC-TEOS is *ca.* 110 nm. In contrast, SiC-C_8 sample gives wider and less intense diffraction peaks, suggesting that the average particle size became smaller (*ca.* 34 nm.) after incorporating the alkyloxysilane. In addition, a low-intensity peak at 33.6° compared with the strong (111) peak is also observed over the pattern of the SiC-C_8 material. According to the literature,[33] this additional peak corresponds to stacking faulty (SF) in the β-SiC structure. The HRTEM image of sample (Fig. 3) provides further evidence to identify the product SiC-TEOS and SiC-C_8 as β-SiC. A perfect arrangement of the atomic layers is observed and the measured distance between the (111) planes is 0.252 nm, very close to the distance between the planes reported in the literature.[6,27]

Fig. 4 shows the representative SEM images of the SiC-TEOS and SiC–C_8 samples. SiC-TEOS consists mainly of ball-like particles with size about 80–400 nm (Fig. 4a), and the larger particles are appeared from agglomeration of the smaller ones. Wei *et al.* suggest the mesopores of SiC synthesized *via* sol–gel method come from the superficial pores on the particles.[22] For SiC–C_8, it is apparent that the particles, with a loose body, are smaller (50–100 nm) than those of SiC-TEOS.

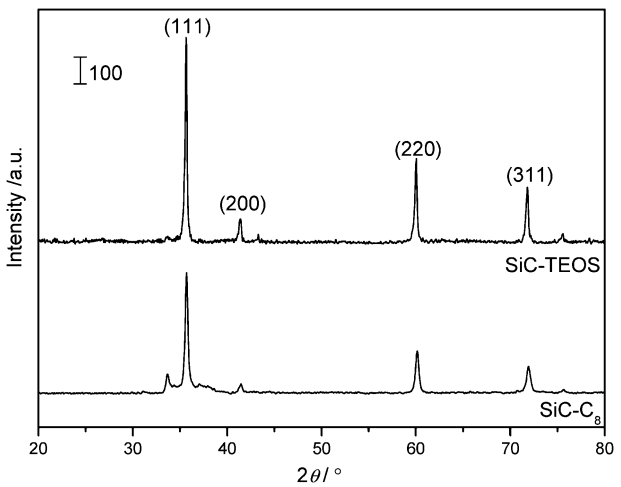

Fig. 2 XRD patterns of SiC-TEOS and SiC-C_8.

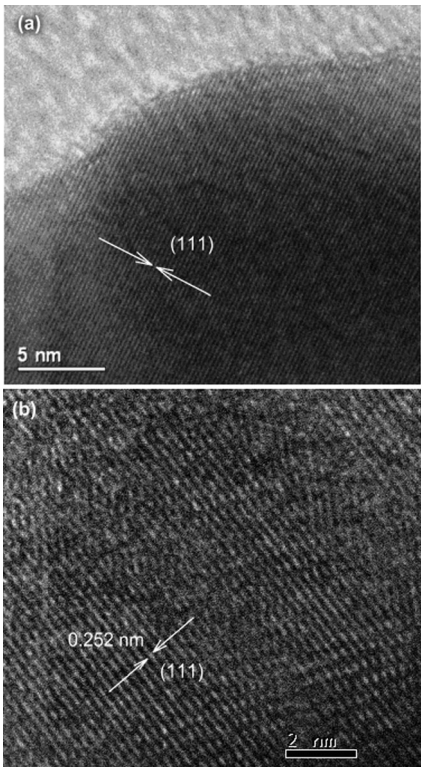

Fig. 3 HRTEM images of SiC-TEOS (a) and SiC-C_8 (b).

XPS was conducted to calculate the composition of surface species of the SiC-C_8 and SiC-C_8-F. As shown in Fig. 5, the surface of the SiC-C_8 is mainly covered by the SiO_2 species (Si 2*p*: 103.4 eV) accompanied by a small amount silicon oxycarbide species (C 1*s*: 285.3 eV),[1,26] only a very few of SiC species (Si 2*p*: 100.8 eV; C 1*s*: 283.5 eV) are exposed. After the washing by HF solution, the SiO_2 and silicon oxycarbide

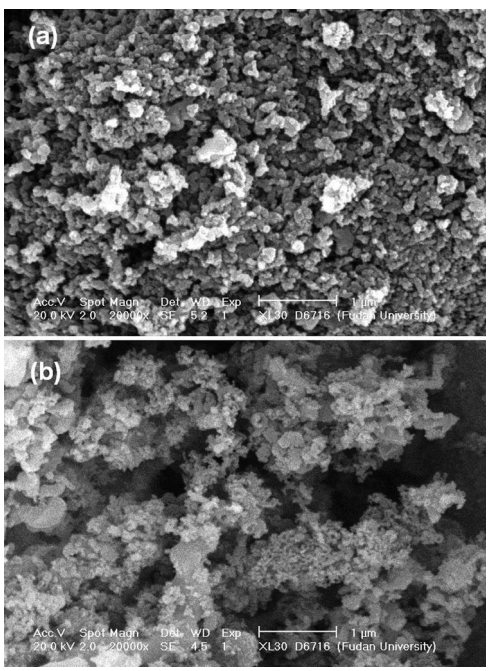

Fig. 4 SEM images of SiC-TEOS (a) and SiC-C_8 (b).

species disappear, and only SiC species are dominating on the surface of SiC-C_8-F. By analysis of the Si, C, and O atom contents (46.7%, 48.2%, and 5.1%, respectively) over SiC-C_8-F sample, the molar ratio of Si/C is 0.97, which is very close to the stoichiometric ratio of SiC. Therefore, it can be concluded that the surface of SiC-C_8 consists mainly of SiO_2 species. Whereas after the washing by HF solution, the SiO_2 film is removed, leaving bare SiC species remaining on the SiC-C_8-F sample.

The mechanism of the conventional synthesis of SiC by sol–gel reaction is described in Scheme 1. Si-OH groups are firstly produced by hydrolysis of Si-OEt groups. Then, Si-O-Si chains are formed by condensation between two Si-OH groups or between a Si-OH group and a Si-OEt group.[33,34] Afterwards, the polymerized Si-O chains form and assemble into the silica matrixes, embedding the sucrose as a carbon source and producing a large amount of SiO_2/C interfaces.[35] Upon heating, the solvent evaporates and the framework of silica gel shrinks into bulky xerogel. During the subsequent carbothermal reaction, SiC is produced in the interface.[36] Finally, SiC materials with porous frameworks are obtained after removing the residual SiO_2 and C.

In contrast with the conventional route, the incorporation of alkyloxysilane with hydrophobic chain can retain its framework during the xerogelation. Meanwhile, the hydrophobic groups serve as additional carbon source.[33] Consequently, the interface between silica and carbon increases drastically and thereby the surface area of final SiC materials is maintained after the carbothermal reduction. Hence, the longer hydrophobic chain of alkyloxysilane, the less shrinkage of the gel and the higher surface area of SiC materials. Indeed, when *n-octyl*-Si$(OEt)_3$ is applied (0.025mol mixed with 0.2 mol TEOS), we observed that the framework of silica demonstrated almost no shrinkage after the xerogelation, in sharp contrast with around 75% shrinkage of volume during the xerogelation of SiC-TEOS.

3.2 Chemical states of V species

H_2-TPR profiles of vanadia loaded catalysts taken at 200–700 °C are presented in Fig. 6. One sharp peak at *ca.* 519 °C is observed on SiC supported samples with low and medium V loadings (0.5 to 1.5 wt%). In the sample with high V content (3.0V-SiC-C_8), the main peak becomes broader and shifted to 557 °C. According to the literature and our previous studies on the reducibility of VO_x/SiO_2 and V-containing mesoporous materials,[28,37,38] the peak at low temperature is attributed to the reduction of highly dispersed tetrahedral vanadia species (VO_4^{3-}), while the peak at *ca.* 557 °C to the reduction of polymeric V^{5+} or bulk-like V_2O_5 species. The progressive shift of the maximum of the H_2 consumption peak to high temperature with the V loading suggests a progressive formation of less reducible highly polymeric vanadia species.

In addition, catalysts with the same V content on different supports (SiC-C_8, SiO_2 and Al_2O_3) are also compared. The profiles for 1.5V-SiC-C_8 sample along with the profiles for 1.5V-SiO_2 and 1.5V-Al_2O_3 catalysts demonstrate a similar temperature maximum (*ca.* 516 °C). This indicates that the surface of these three catalysts is dominated by the highly dispersed tetrahedral vanadia species. However, for 1.5V-SiC-C_8-F, the reduction peak shifts to much higher temperature (560 °C), along with a second band in 580–650 °C, suggesting that the surface of 1.5V-SiC-C_8-F sample is dominated by highly polymeric $(VO_4^{3-})_x$ units or bulk-like V_2O_5 species. It implies, due to the exterior dominating SiC species and thus weak interaction between metal oxide and SiC surface,[12,39] the pure SiC surface of SiC-C_8-F is not favorable for the high dispersion of the vanadia species.

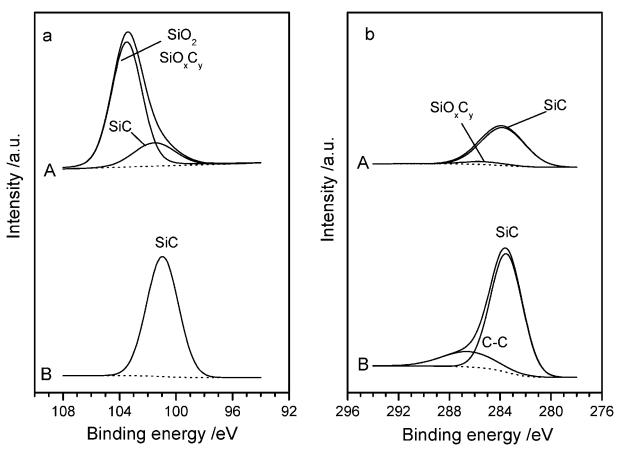

Fig. 5 XPS spectra of Si 2*p* (a) and C 1*s* (b) for SiC-C_8 (A) and SiC-C_8-F (B).

3.3 Catalytic tests for ODH of propane

Propylene is a major building block of the modern petrochemical industry and is extensively used for the manufacture of diverse products ranging from solvents to plastics.[40,41] In practical industrial processes, propylene is mainly produced by steam cracking or a direct dehydrogenation of various hydrocarbon feedstocks at high temperatures, where intensive energy consumption and coking present serious problems.[29,42] With the constantly growing propylene market and rapidly rising fuel costs, the catalytic ODH of propane has attracted tremendous recent attention owing to the absence of detrimental thermodynamic limitations and lower operation temperatures.[43,44] A wide range of catalysts have been reported for ODH of propane and therein the supported vanadia catalysts,[45] *e.g.* V_2O_5/SBA-15,[28,46] V_2O_5/ITQ-6,[47] and V_2O_5/TiO_2,[48] have been considered to be most active and selective for the process.

In the present study, owing to it having the highest surface area, SiC-C_8 was chosen as support to load vanadia and used for the ODH of propane. The catalytic results of the V-SiC catalysts are shown in Table 2. Blank results show that negligible homogenous reaction could occur under the reaction conditions employed here and the V-free SiC-C_8 gives very poor catalytic activity. The introduction of V greatly increases propane conversion. For all the V-SiC catalysts, propylene and CO_x are the main products, accompanied by small amounts of C_2H_4, CH_4 and oxygenates. Similar catalytic behavior has been observed over vanadia catalysts supported on mesoporous silicas.[29,37]

As widely reported, the catalytic behavior of supported vanadia catalysts in the selective oxidation of light alkanes

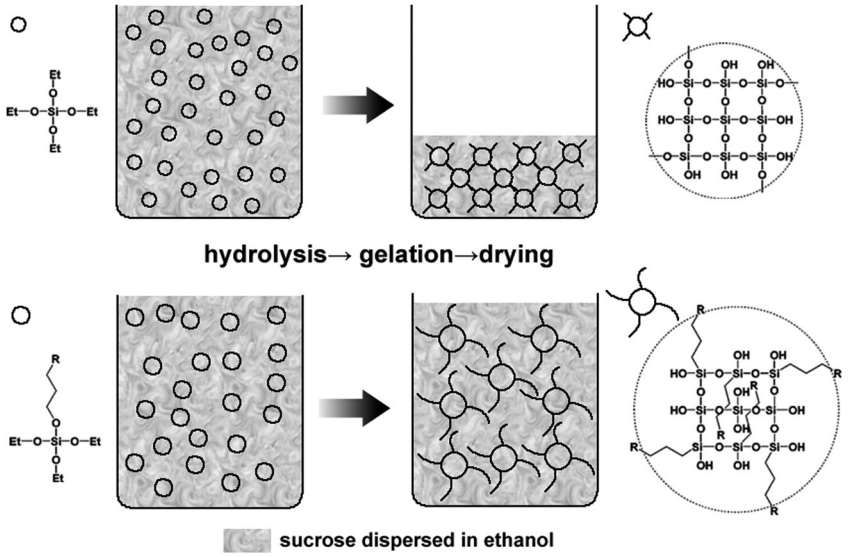

Scheme 1 Proposed mechanism of the formation of mesostructured SiC *via* the conventional (a) and hybrid sol–gel (b) methods.

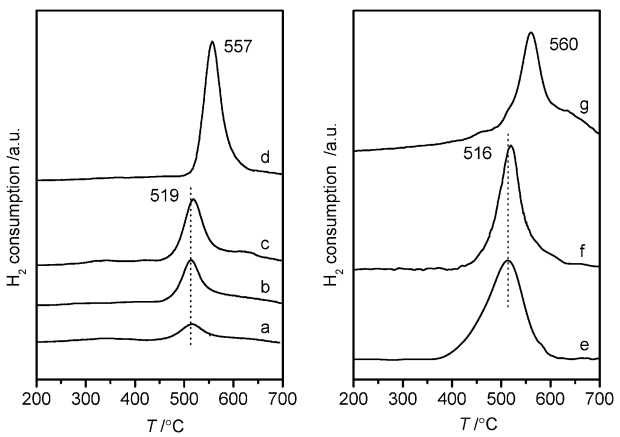

Fig. 6 TPR profiles of V-supported catalysts: (a) 0.5V-SiC-C_8 (b) 1.0V-SiC-C_8 (c) 1.5V-SiC-C_8 (d) 3.0V-SiC-C_8 (e) 1.5V-Al_2O_3 (f) 1.5V-SiO_2 (g) 1.5V-SiC-C_8-F.

depends strongly on the dispersion of vanadia loaded on the supports.[41,49–51] The highly dispersed and isolated tetrahedral vanadia species (VO_4^{3-}) containing terminal V=O groups have been suggested as the active sites for the selective formation of propylene.[50,52] The results reported in Table 2 point to a marked composition effect on the catalytic performance of the V-SiC catalysts. The catalysts loaded with medium V content (1.0 to 1.5 wt%) demonstrate an enhanced catalytic performance in the ODH of propane to propylene. This fact is apparently related to the aforementioned H_2-TPR results. Additionally, it is found that the selectivity to propylene decreases while the propane conversion increases with the increase of V loading. The highest propylene yield of 20.1% is obtained over the 1.5V-SiC-C_8 catalyst, affording a high space-time yield (STY_{C3H6}) of 2.27 kg kg $_{cat}^{-1}$ h^{-1}.

Besides, it is clear that the 1.5V-SiC-C_8 exhibited much higher propane conversion and selectivity to propylene than those of 1.5V-SiO_2, 1.5V-Al_2O_3, and 1.5V-SiC-C_8-F catalysts. To further understand the activation of propane on the different catalysts in more real conditions, the variation of the selectivity to propylene, which changed with the propane conversion, was studied during the ODH of propane on these catalysts. As shown in Fig. 7, the selectivity to propylene decreases with the increase of conversion on all catalysts. However, at the same propane conversion level, the 1.5V-SiC-C_8 catalyst exhibits higher selectivity to propylene than 1.5V-SiO_2 and 1.5V-Al_2O_3 catalysts. Considering that the surface of

Table 2 Catalytic performances of vanadia catalyst

		S (%)					
Sample	*C* (C_3H_8)[a] (%)	C_3H_6	C_2H_4	CH_4 and oxygenates[b]	CO_x	*Y* (C_3H_6) (%)	$STY(C_3H_6)$[c] /kg kg_{cat}^{-1} h^{-1}
SiC-C_8	3.7	57.7	13.9	6.9	21.5	2.1	0.24
3.0V-SiC-C_8	29.2	54.7	13.9	7.3	24.1	16.0	1.80
1.5V-SiC-C_8	32.5	62.1	16.8	5.5	15.6	20.2	2.27
1.0V-SiC-C_8	26.5	65.1	14.1	5.0	15.8	17.3	1.95
0.5V-SiC-C_8	18.3	66.1	16.3	7.1	10.5	12.1	1.36
1.5V-SiC-C_8-F	32.8	39.2	10.0	15.3	35.5	12.9	1.45
1.5V-SiO_2	27.0	51.0	8.9	6.0	34.1	13.8	1.55
1.5V-Al_2O_3	25.1	47.8	3.5	1.3	47.4	12.0	1.35

[a] Reaction condition: $W_{cat.}$ = 50 mg, 600 °C, $C_3H_8/O_2/N_2$ = 1/1/4 (total flow rate = 30 mL min^{-1}), all activity data are collected after the reaction time of 1 h. [b] Partial oxygenated products, *i.e.*, acrolein. [c] Space-time yield of propylene.

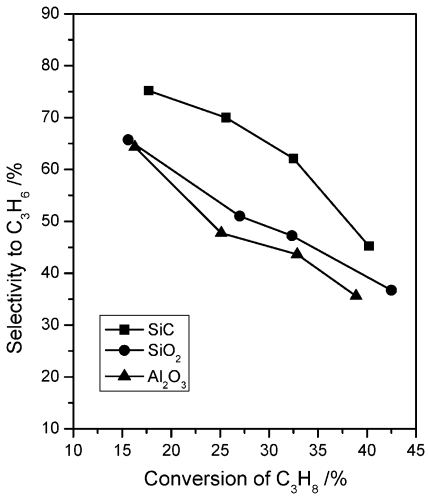

Fig. 7 Selectivity to propylene *versus* propane conversion on various supports with a similar V loading.

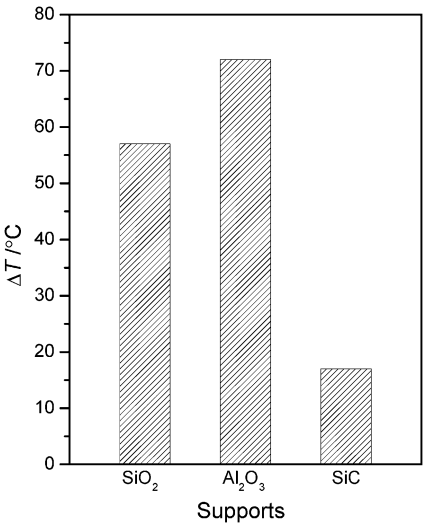

Fig. 8 Difference of set temperature and catalyst bed's inner temperature for various supports.

the SiC-C_8 material is actually composed of silica as revealed by XPS results, it is interesting to compare the catalytic performances among various silica-loaded vanadia catalysts. Table S1† lists the performances of vanadia supported on the several reported porous silica materials. It should be noted that the catalytic conditions, *e.g.* reaction temperature and space velocity for the ODH of propane, may deviate from each other. Nevertheless, a rough comparison is still feasible in the present study. Obviously, the other reported silica-based supports possess significantly larger surface areas than the SiC-C_8, favoring higher dispersion of vanadia species and improving of selectivity to propylene. However, it is remarkable that the selectivity obtained is appreciably less than that of 1.5V-SiC-C_8. This indicates that, concerning the effect of catalytic support, there is a more important factor outweighing the surface area and porosity to control, or at least influence, the selectivity to the target molecule in the reaction.

The ODH of propane is highly exothermic, both for the production of the desired product, propylene, and for its parallel full oxidation reaction.[49,53] During the oxidation procedure, hot spots or temperature runaway[54,55] can occur over the catalysts due to the poor thermal conductivity (Table 3) of the conventional supports such as SiO_2 and Al_2O_3.[56] SiC material has been long known to be one of the most promising materials for high-temperature structural applications, especially due to its high thermal conductivity, which should greatly contribute to the heat management of the reaction.[7,9] To detect the hot spots effect during the ODH of propane reactions, the temperature profiles of the catalytic system were measured during the reaction.

Table 3 Thermal conductivity of catalyst supports

Support	Thermal conductivity[9]/W m^{-1} K^{-1}
SiO_2	0.015–1
Al_2O_3	1–8
Si_3N_4	6
BN	31
SiC	146–270

Herein, the difference (ΔT) of catalyst bed's inner temperature (T_{bed}) and the set temperature (T_{set}) is plotted comparatively in Fig. 8. ΔT over the 1.5V-Al_2O_3 and 1.5V-SiO_2 catalysts are higher than 55 °C, which implies that obvious hot spots effect occurs during the catalytic reactions. Indeed, when much higher GHSV (Gas Hourly Space Velocity; 1000 mL min^{-1} $g_{catal.}^{-1}$) was applied, the hot spots effect occurred more seriously, where the ΔT would be up to 120 °C. Interestingly, the ΔT acquired over the 1.5V-SiC-C_8 catalyst is very low. This can contribute to the superior higher propylene selectivity over the 1.5V-SiC-C_8 catalyst to those acquired over the 1.5V-Al_2O_3 and 1.5V-SiO_2 catalyst under the same propane conversion level, although the dispersion of vanadia species is similar over these three catalysts.

In the case of the 1.5V-SiC-C_8 and 1.5V-SiC-C_8-F catalysts, although they possessed similar thermal conductivity, 1.5V-SiC-C_8-F exhibits appreciably lower propylene selectivity (See Table 1). The different catalytic behaviors can be explained according to the nature of the surface of the SiC materials. After SiC-C_8 material was washed with HF solution for the second time, the superficial silica film was removed thoroughly and the surface of SiC-C_8-F became almost chemically inert. This results in less dispersion of vanadia species and therein lower selectivity to propylene since the highly-polymeric $(VO_4)_x$ species would favor consecutive oxidation of propylene in ODH of propane. At this juncture, it can be confirmed that the silica film plays a key role in benefiting the vanadia species dispersion and improving the catalytic performance.

4. Conclusions

We have developed a novel hybrid sol–gel approach for the practical synthesis of high surface area mesostructured SiC with well-developed and tunable porosity. The key to obtaining these structures is the formation of a mesostructured hybrid xerogel, obtained through the sol–gel processing of TEOS in the presence of appropriate amount of alkyloxysilane with varying alkyl-chain lengths, and the mesostructures could

be largely maintained after the subsequent carbothermal reduction treatment. The surface areas increase consistently with the chain lengths of the alkyloxysilane, showing the importance of alkyloxysilane in the formation of these mesostructures. The optimum synthesis is achieved by using proper amount of *n*-octyl-Si(OEt)$_3$ as the alkyloxysilane precursor, which can afford the synthesis of a SiC-C$_8$ with a high surface area of *ca.* 345 m^2 g^{-1}. The applicability of the present SiC-C$_8$ material is highlighted by the ODH of propane to propylene using vanadia supported on the as-synthesized SiC-C$_8$, which show far superior performance in terms of higher selectivity to propylene at high propane conversion levels than those with on conventional Al_2O_3 or SiO_2 supports.

Acknowledgements

This work was financially supported by the National Natural Science Foundation of China (20633030, 20721063, 20803012 and 20873026), the National High Technology Research and Development Program of China (2066AA03Z336), the National Basic Research Program of China (2009CB623506), Science & Technology Commission of Shanghai Municipality (08DZ2270500), and Shanghai Education Committee (06SG03).

References

1 Z. X. Yang, Y. D. Xia and R. Mokaya, *Chem. Mater.*, 2004, **16**, 3877.
2 G. H. Liu, K. Yang, J. T. Li, K. Yang, J. S. Du and X. Y. Hou, *J. Phys. Chem. C*, 2008, **112**, 6285.
3 A. H. Lu, W. Schmidt, W. Kiefer and F. Schuth, *J. Mater. Sci.*, 2005, **40**, 5091.
4 H. Yamashita, Y. Nishida, S. Yuan, K. Mori, M. Narisawa, Y. Matsumura, T. Ohmichi and I. Katayama, *Catal. Today*, 2007, **120**, 163.
5 N. Keller, V. Keller, F. Garin and M. J. Ledoux, *Mater. Lett.*, 2004, **58**, 970.
6 X. N. Shen, Y. Zheng, Y. Y. Zhan, G. H. Cai and Y. H. Xiao, *Mater. Lett.*, 2007, **61**, 4766.
7 W. Z. Sun, G. Q. Jin and X. Y. Guo, *Catal. Commun.*, 2005, **6**, 135.
8 C. Vix-Guterl, I. Alix, P. Gibot and P. Ehrburger, *Appl. Surf. Sci.*, 2003, **210**, 329.
9 M. J. Ledoux and C. Pham-Huu, *CATTECH*, 2001, **5**, 226.
10 F. Moreau and G. C. Bond, *Catal. Commun.*, 2007, **8**, 1403.
11 L. Pesant, J. Matta, F. Garin, M. J. Ledoux, P. Bernhardt, C. Pham and C. Pham-Huu, *Appl. Catal., A*, 2004, **266**, 21.
12 Q. Wang, W. Z. Sun, G. Q. Jin, Y. Y. Wang and X. Y. Guo, *Appl. Catal., B*, 2008, **79**, 307.
13 C. Pham-Huu, N. Keller, G. Ehret and M. J. Ledoux, *J. Catal.*, 2001, **200**, 400.
14 P. Nguyen, D. Edouard, J. M. Nhut, M. J. Ledoux, C. Pham and C. Pham-Huu, *Appl. Catal., B*, 2007, **76**, 300.
15 C. Pham-Huu, P. Delgallo, E. Peschiera and M. J. Ledoux, *Appl. Catal., A*, 1995, **132**, 77.
16 M. J. Ledoux, C. Crouzet, C. Pham-Huu, V. Turines, K. Kourtakis, P. L. Mills and J. J. Lerou, *J. Catal.*, 2001, **203**, 495.
17 G. Winé, M. J. Ledoux and C. Pham-Huu, *Top. Catal.*, 2007, **45**, 111.
18 P. Krawiec, D. Geiger and S. Kaskel, *Chem. Commun.*, 2006, 2469.
19 R. Moene, M. Makkee and J. A. Moulijn, *Appl. Catal., A*, 1998, **167**, 321.
20 O. Yamada, Y. Miyamoto and M. Koizumi, *J. Mater. Res.*, 1986, **1**, 275.
21 C. W. Zhu, G. Y. Zhao, V. Revankar and V. Hlavacek, *J. Mater. Sci.*, 1993, **28**, 659.
22 Y. Zheng, Y. Zheng, L. X. Lin, J. Ni and K. M. Wei, *Scr. Mater.*, 2006, **55**, 883.
23 X. Y. Guo and G. Q. Jin, *J. Mater. Sci.*, 2005, **40**, 1301.
24 J. H. Eom, Y. W. Kim, I. H. Song and H. D. Kim, *J. Eur. Ceram. Soc.*, 2008, **28**, 1029.
25 Y. F. Shi, Y. Meng, D. H. Chen, S. J. Cheng, P. Chen, H. F. Yang, Y. Wan and D. Y. Zhao, *Adv. Funct. Mater.*, 2006, **16**, 561.
26 Z. C. Liu, W. H. Shen, W. B. Bu, H. R. Chen, Z. L. Hua, L. X. Zhang, L. Li, J. L. Shi and S. H. Tan, *Microporous Mesoporous Mater.*, 2005, **82**, 137.
27 J. Yan, A. Wang and D.-P. Kim, *J. Phys. Chem. B*, 2006, **110**, 5429.
28 Y. M. Liu, Y. Cao, N. Yi, W. L. Feng, W. L. Dai, S. R. Yan, H. Y. He and K. N. Fan, *J. Catal.*, 2004, **224**, 417.
29 J. Xu, M. Chen, Y. M. Liu, Y. Cao, H. Y. He and K. N. Fan, *Microporous Mesoporous Mater.*, 2009, **118**, 354.
30 J. Xu, L. C. Wang, Y. M. Liu, Y. Cao, H. Y. He and K. N. Fan, *Catal. Lett.*, 2009, **133**, 307.
31 G. Q. Jin and X. Y. Guo, *Microporous Mesoporous Mater.*, 2003, **60**, 207.
32 P. Krawiec and S. Kaskel, *J. Solid State Chem.*, 2006, **179**, 2281.
33 Y. M. Z. Ahmed and S. M. El-Sheikh, *J. Am. Ceram. Soc.*, 2009, **92**, 2724.
34 C. J. Brinker and G. W. Scherer, *Sol–gel science: the physics and chemistry of sol–gel processing*, Academic Press, Inc., San Diego, 1990.
35 X. Y. Guo, G. Q. Jin and Y. J. Hao, Morphology-controlled synthesis of nanostructured silicon carbide, *Silicon Carbide 2004-Materials: Processing and Devices*, 2004, **815**, 77.
36 C. Vix-Guterl, I. Alix and P. Ehrburger, *Acta Mater.*, 2004, **52**, 1639.
37 B. Solsona, T. Blasco, J. M. L. Nieto, M. L. Pena, F. Rey and A. Vidal-Moya, *J. Catal.*, 2001, **203**, 443.
38 F. Ying, J. H. Li, C. J. Huang, W. Z. Weng and H. L. Wan, *Catal. Lett.*, 2007, **115**, 137.
39 R. Shang, Y. Wang, G. Jin and X. Y. Guo, *Catal. Commun.*, 2009, **10**, 1502.
40 A. Adamski, Z. Sojka, K. Dyrek, M. Che, G. Wendt and S. Albrecht, *Langmuir*, 1999, **15**, 5733.
41 F. Cavani, N. Ballarini and A. Cericola, *Catal. Today*, 2007, **127**, 113.
42 B. Frank, A. Dinse, O. Ovsitser, E. V. Kondratenko and R. Schomäcker, *Appl. Catal., A*, 2007, **323**, 66.
43 M. M. Bhasin, J. H. McCain, B. V. Vora, T. Imai and P. R. Pujado, *Appl. Catal., A*, 2001, **221**, 397.
44 S. Vajda, M. J. Pellin, J. P. Greeley, C. L. Marshall, L. A. Curtiss, G. A. Ballentine, J. W. Elam, S. Catillon-Mucherie, P. C. Redfern and F. Mehmood, *Nat. Mater.*, 2009, **8**, 213.
45 A. Klisinska, K. Samson, I. Gressel and B. Grzybowska, *Appl. Catal., A*, 2006, **309**, 10.
46 Y. M. Liu, Y. Cao, K. K. Zhu, S. R. Yan, W. L. Dai and K. N. Fan, *Chem. Commun.*, 2002, **2002**, 2832.
47 B. Solsona, J. M. L. Nieto and U. Diaz, *Microporous Mesoporous Mater.*, 2006, **94**, 339.
48 A. A. Lemonidou, L. Nalbandian and I. A. Vasalos, *Catal. Today*, 2000, **61**, 333.
49 K. Chen, A. Khodakov, J. Yang, A. T. Bell and E. Iglesia, *J. Catal.*, 1999, **186**, 325.
50 A. Khodakov, B. Olthof, A. T. Bell and E. Iglesia, *J. Catal.*, 1999, **181**, 205.
51 D. A. Bulushev, L. Kiwi-Minsker, F. Rainone and A. Renken, *J. Catal.*, 2002, **205**, 115.
52 Y. Wang, Q. H. Zhang, Y. Ohishi, T. Shishido and K. Takehira, *Catal. Lett.*, 2001, **72**, 215.
53 K. Chen, E. Iglesia and A. T. Bell, *J. Phys. Chem. B*, 2001, **105**, 646.
54 S. L. Liu, G. X. Xiong, H. Dong and W. S. Yang, *Appl. Catal., A*, 2000, **202**, 141.
55 V. L. Barrio, G. Schaub, M. Rohde, S. Rabe, F. Vogel, J. F. Cambra, P. L. Arias and M. B. Gumez, *Int. J. Hydrogen Energy*, 2007, **32**, 1421.
56 H. Liu, S. Li, S. Zhang, J. Wang, G. Zhou, L. Chen and X. Wang, *Catal. Commun.*, 2008, **9**, 51.

